Steel Pipe Measurement System Based on Laser Rangefinder

Federico Cavedo, Michele Norgia, Senior Member, IEEE, Alessandro Pesatori, Member, IEEE, and Gabriel E. Solari

***Abstract*— In order to improve the quality of steel pipes, one of the main requisites is to build pipes that are as close as possible to the designed one. To accomplish this task, an optical distance sensor of reduced size and very low power consumption was developed inside a measurement system allowing reconstruction of steel pipe dimensions. The results obtained led to the construction of a working prototype configured as an active triangulation rangefinder with a gamut of 10 cm starting at 5 cm. The characterization of the novel rangefinder has confirmed the feasibility of this new system with a resolution of ∼10 μm on a range of measurement of 10 cm, providing up to 10 000 measurements per second.**

***Index Terms*— Industrial control, measurement by laser beam, optical sensors, position measurement, semiconductor lasers.**

I. Introduction

ACCURATE determination of the size of objects under inspection is important to ensure high product quality in some manufacturing companies. The distance optical measurement devices are widely used today in industry [1]–[3]. There are many applications where it is crucial to measure some parameters of interest without having to come into contact with the object under examination. Some optical techniques enable us to carry out these measurements very fast and reliably.

The purpose of this work was to develop an optical distance sensor that can be used as a measuring system for characterizing the profile of steel tubes in an industrial environment [4]. In order to ensure less defects and imperfections in a pipe, it is very important to know accurately the tube profile, especially on the edge where the pipe is typically soldered.

A wide range of optical sensors [4]–[10] of position and distance with micrometer resolution and very high accuracy are commercially available; however, industrial application requires an *ad hoc* product with some stringent specifications. The instrument required should be small, not more than 5 cm wide and 4 cm long, light, and consume very low power, less than 50 mA at 3.3 V. It should also operate properly with a resolution of ∼10 μm on a 10-cm range and up to a temperature of 60 °C in order to be used on a steel pipe production line.

Manuscript received June 30, 2015; revised December 10, 2015; accepted December 11, 2015. The Associate Editor coordinating the review process was Dr. George Xiao.

F. Cavedo, M. Norgia, and A. Pesatori are with the Dipartimento di Elettronica, Informazione e Bioingegneria, Politecnico di Milano, Milan 20133, Italy (e-mail: alessandro.pesatori@polimi.it).

G. E. Solari is with the Dalmine S.P.A., Dalmine 24044, Italy (e-mail: gsolari@tenaris.com).

Color versions of one or more of the figures in this paper are available online at http://ieeexplore.ieee.org.

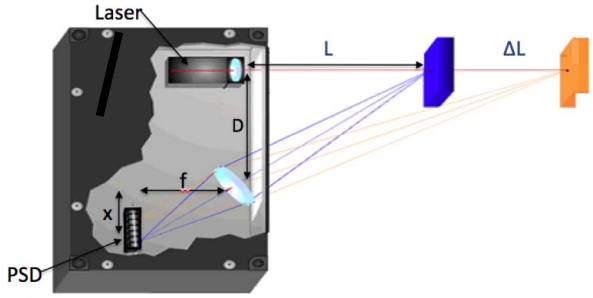

Fig. 1. Geometric schematic of the laser rangefinder.

A sensor with all these characteristics is not currently available on the market and in this paper first the feasibility of the requests is discussed and how to accomplish such specifications is then figured out.

The project led to the realization of a working prototype of a sensor characterized by its compact size and low consumption. The design choices and the results obtained so far are presented in this paper, which is organized as follows.

In the following section, a sketch of the measurement system and the design specifications and a brief theoretical introduction of the sensor principles of measurements are presented. The design of the electronics for the acquisition and postprocessing of the sensor signals will be discussed in the third section, which will be followed by the first experimental verification of the feasibility of the instrument. In the conclusion section, the improvements and some possible future developments will be presented.

II. Measurement Instrument Design

The design of the rangefinder was based on the classical simple model shown in Fig. 1 [11].

The image represents the schematic of a triangulation measurement device, where D is the distance between the laser and the optical center of the position sensor detector (PSD), f is the distance between the PSD and the lens used to focus the light, and α is the angle of inclination of the receiving lens [12]. This configuration is slightly different from the most common configuration for a laser triangulation device due to the tilt of the lens with respect to the beam of light projected on the object in order to reduce any bias caused by the angle of incidence of the light on the lens. With respect

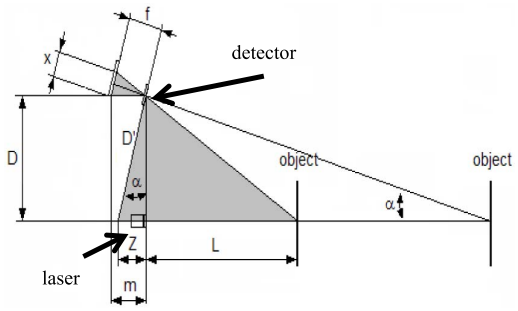

Fig. 2. Schematic of the laser rangefinder.

to the variable defined in Fig. 2, the equation that relates the object distance L to the position x of the laser spot on the detector is [6], [12], [13]

$$L = \frac{D \cdot f}{\cos^2(\alpha)} \cdot \frac{1}{x} = D \cdot \tan(\alpha). \tag{1}$$

From (1), it is clear that the relation between the distance of the object and the measurement variable x is inherently nonlinear. The aspects to be considered when deciding the geometry of the head of the rangefinder and then the parameters D, f, and α are the measurement range required, the length of the active area of the PSD, the maximum size of the instrument, and the resolution you want obtained in the range of measurement.

In order to achieve a measurement range between 5 and 15 cm, it was decided to use a PSD with an active area of 6 mm (First Sensor, mod. OD6-6-SO16). In addition, it was requested that the distance between the laser and the PSD not exceed 4 cm and the resolution on the measurement be $\sim$10 μm.

Starting from (1), it is possible to obtain the first condition with the parameters D, f, and α so that it can detect changes at a distance in the range from $L_{\min}$ to $L_{\max}$ with a 6-mm-long PSD

$$(x_{\max} - x_{\min}) < 6 \text{ mm} \tag{2}$$

$$x_{\max} = \frac{D \cdot f}{(L_{\max} + D \cdot \tan(\alpha)) \cdot \cos^2(\alpha)} \tag{3}$$

$$x_{\max} = \frac{D \cdot f}{(L_{\max} + D \cdot \tan(\alpha)) \cdot \cos^2(\alpha)}. \tag{4}$$

The resolution of the system is also a function of the achievable resolution to detect the position x of the laser spot on the sensor and then the geometry of the system. Differentiating (1) with respect to the variable x, we get

$$\frac{dL}{dx} = \frac{D \cdot f}{\cos^2(\alpha)} \cdot \frac{1}{x^2}. \tag{5}$$

Starting from (5), we can finally go back and then obtain the resolution of the sensor, and by knowing the geometric parameters of the rangefinder, choose a resolution at a fixed distance

$$|\Delta x| = \frac{\Delta L \cdot \cos^2(\alpha) \cdot x^2}{D \cdot f}. \tag{6}$$

TABLE I
GEOMETRY OF THE RANGEFINDER

D	30 mm
f	13.5 mm
α	15°
L	50-150 mm

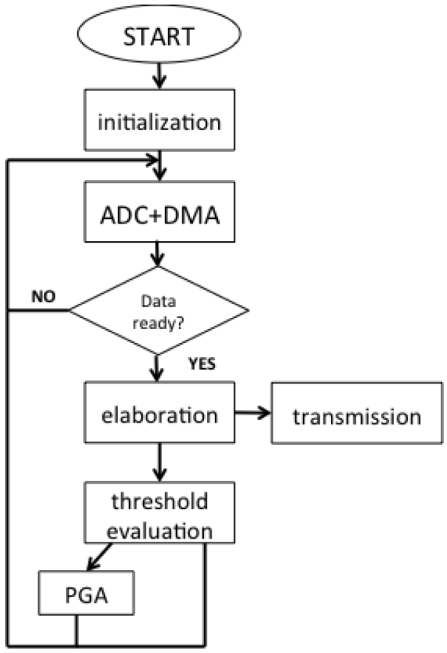

Fig. 3. Flowchart of the rangefinder method of measurement.

On the basis of our parameters: a range of 10 cm and a resolution not worse than 10 μm on the all range, we chose these values.

Table I summarizes the geometrical parameters chosen for the sensor. Note that the focal length of the lens was chosen in such a way that it satisfied the relationship

$$\frac{1}{p} + \frac{1}{q} = \frac{1}{f} \tag{7}$$

when the object is at a distance of $q = 15$ cm, using a lens with a focal length of, $f = 13.5$ mm, the image is formed at a distance of $p = 15$ mm from the lens and on the plane of the PSD. In this way, the more nonlinear the curve of measurement of the rangefinder becomes, the smaller the laser spot will be.

III. HARDWARE SETUP

The signal on the PSD is read in current through a transimpedance circuit to avoid possible problems of linearity due to the logarithmic relationship between the voltage and the current of the PSD that acts as a photodiode [1].

Another caution in reading the PSD was to force the bias reverse voltage constant and approximately equal to zero. This is done in order to minimize the dark current and the noise; in fact, as it can be observed in Fig. 3, the cathode is connected at 2.5 V and the anodes of the PSD are connected to

the nodes of the virtual ground of two operational amplifiers working as transimpedance amplifiers. The outputs of the two transimpedance amplifiers are amplified again to be acquired by an analog-to-digital converter inside a microcontroller (STMicroelectronics, STM32F303).

The STM32F303 puts together a 32-bit ARM Cortex-M4 core with an operating frequency of 72 MHz and integrated analog peripherals, enabling low-cost and low-complexity practical features such as fast (<30 ns) comparators, operational amplifiers with programmable gain, a 12-bit DAC, and a 12-bit ADC with a frequency of 3.4 Msample/s per channel (maximum sampling frequency, when the main clock is set to 72 MHz). The four operational amplifiers are very important, because they allow the implementation of the variable gain in a compact and simple way, which is very useful for this application.

The purpose of this additional amplification on the transimpedance signal is to use the whole range of the ADC, overcoming the problems of reflectivity variation of the surface to be measured. The outputs of this further gain stage are directly connected to the ADC, where it will start the phase of acquisition and elaboration as explained in the flowchart of Fig. 3. In order to program the microcontroller, a MDK Microcontroller Development Kit (Keil) was used in C++ language. The program is a simple finite state machine in order to obtain measurements as fast as possible.

Without this automatic gain control, there would be an additional dependence of the signal from the distance; due to the significant reduction of the signal transmitted by reception optics when the object is very close to the maximum of the range (the attenuation is almost quadratic with the distance). The use of gain control reduces the relative quantization noise and the influence of disturbances generated by the microcontroller.

This algorithm of elaboration is decisive for the stability and repeatability of the measurement because, like every system based on triangulation, the way in which the incident light is reflected from the surface may greatly influence the measurement repeatability, since small variations of the signal magnitudes can imply a significant change in the distance measured. How the characteristics of the target can alter the measurement was considered for deep study. The pipes are typically made of a black metal and do not work as perfect diffusers, so it is important to precisely characterize this kind of surface in order to make an accurate dimensional measurement.

The laser diode is pulsed at a frequency of 10 kHz with a duty cycle of 10%, in order to limit the power consumption and filter the ambient light through a synchronous detection. The timing is completely driven by the microcontroller. For each pulse, it acquires 13 samples before, 26 samples during the pulse, and 13 samples after, at a sampling frequency of 3.4 MHz. The amplitude of each pulse is calculated as the difference between the means of the upper and the lower points. In this way, we implement a strong filtering of the ambient light and also of all the spurious signals (not synchronous with the pulses). The sampling rate is at a frequency greater than the Nyquist one (the analog bandwidth

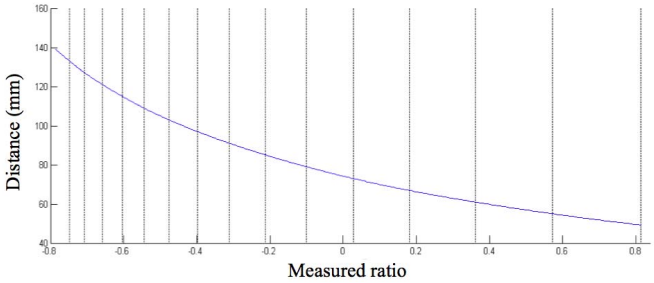

Fig. 4. Measured voltage ratio versus distance.

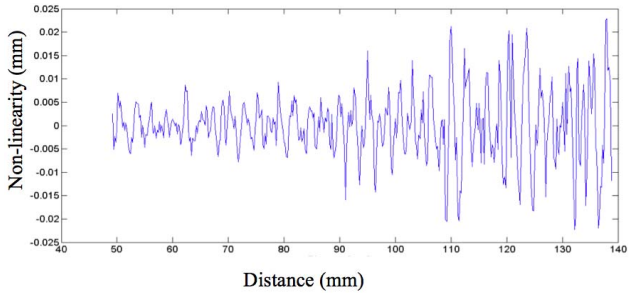

Fig. 5. Calculated nonlinearity varying the target distance after the calibration.

is about 1 MHz) in order to better filter the noise and obtain an SNR that is the greatest possible.

After acquiring the two pulses at the output of the transimpedance amplifiers, the ratio between their difference and sum is calculated [1]. This voltage ratio (difference/sum) is measured at different distances in order to calibrate the instrument.

The theory on the geometry of the optical head indicates a hyperbolic relationship between distance from the target and displacement on the PSD, but the real transduction curve can be quite different. It is due to factors such as the nonlinearity of the PSD (whose error is minimum at the center and maximum at the extremes) and the inclination of the board with respect to the light beam. The calibration was done placing the rangefinder on a mechanical linear translation stage moving it at steps of 5 μm from a black (anodized) metal target starting from 5 mm till 140 mm. Fig. 4 shows the measured transduction curve. In order to calibrate the rangefinder, the curve voltage measured ratio (difference/sum) versus $1/L$ has been interpolated with a fifth-order polynomial, but the results were still not satisfactory. Therefore, it was decided to do an interpolation of the curve dividing it in some small windows to get a better fitting.

For the evaluation and selection of the fitting, an algorithm was created in MATLAB that was tested for different combinations of windows and order of fitting polynomial; observing the graphs of nonlinearity, where we marked the sections of the feature, it was possible to assess whether the peaks that arose were due to the jumps of the window or not.

Finally, after evaluating the possible combinations, we find the best solution, which consists in dividing the curve into 100 intervals, and calculate the regression curve of fifth order for each interval.

Fig. 5 shows the differences between the measurement of the calibrated sensor and the real distance. As it can be

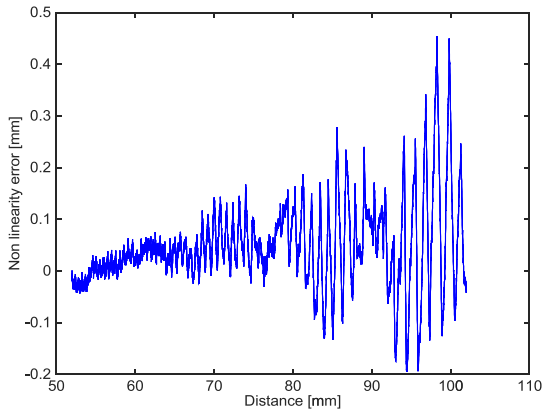

Fig. 6. Measured nonlinearity of the commercial rangefinder.

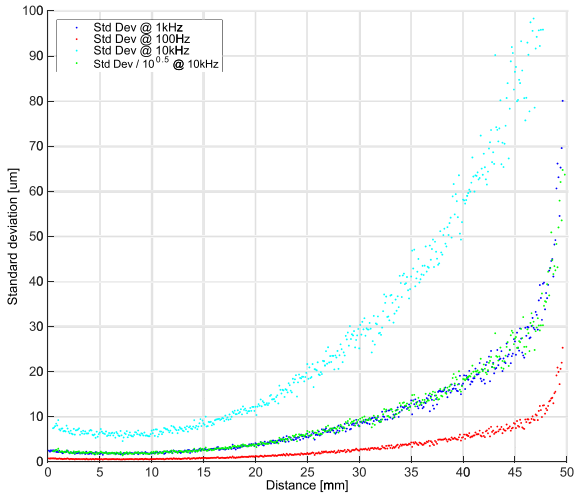

Fig. 7. Standard deviation of the instrument calculated at different frequencies of measurement: 100 Hz, 1 kHz, and 10 kHz at different distances and the uncertainty calculated on ten measurements.

seen from Fig. 5, while increasing the distance, the error of measurement grows up, measured by the difference from the real distance. The results were very satisfactory compared with the results obtained with the commercial instruments shown in Fig. 6. These kinds of instruments reach an error of 400 μm, which is not compatible with the requested resolution.

The good quality of the measurement is confirmed by the standard deviation measured through all the characterization of the rangefinder shown in Fig. 7. It is clear that increasing the velocity of the measurement worsens the results, but the standard deviations are always acceptable for the specific application.

IV. Circular Pipes Reconstruction

The main issue is to measure the circularity of the pipes, compensating for the fact that the measurement system will be somehow out of axis. The aim of this section is to find a mathematical expression to compensate for the errors due to a distance r_e of the rotor axis relative to the axis of rotation, but assuming that the axes are parallel to each other.

We have to find the intersection of the circle expressed in terms of $\varphi = \omega t$ with the abscissa axis from the side of

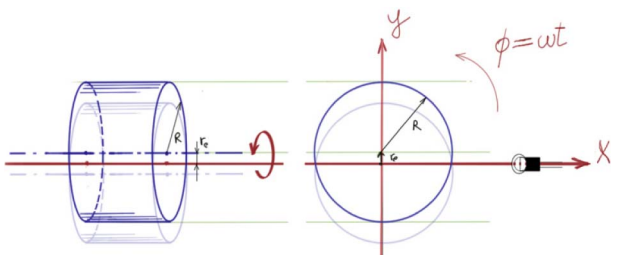

Fig. 8. Problem of the cylinder out of axis.

the sensor. Proceeding in this way, we would get (less than a constant) expression of the signal distance we should expect from the sensor.

We are interested in finding a solution to the system of the following equations:

$$x^2 + y^2 = R^2. \tag{8}$$

During the rotation, the center of the cylinder describes a circle in the section shown on the right in Fig. 8 with radius r_e. For this reason, the center of the circle of the cylinder will have the coordinates

$$h = r_e \cos\varphi, \quad k = r_e \sin\varphi. \tag{9}$$

To derive the equation of any geometric shape after a counterclockwise rotation with angle φ, the matrix should be called rotation to the vector (x, y) for each point, namely

$$\begin{pmatrix} x' \\ y' \end{pmatrix} = \begin{pmatrix} \cos\varphi & \sin\varphi \\ -\sin\varphi & \cos\varphi \end{pmatrix} \begin{pmatrix} x \\ y \end{pmatrix}. \tag{10}$$

Applying the second and the third equation of the circle, we obtain

$$[(x-h)\cos\varphi + (y-k)\sin\varphi]^2 + [(y-k)\cos\varphi - (x-h)\sin\varphi]^2 = R^2 \tag{11}$$

$$[x\cos\varphi - h\cos\varphi + y\sin\varphi - k\sin\varphi]^2 + [y\cos\varphi - k\cos\varphi + x\sin\varphi - h\sin\varphi]^2 = R^2. \tag{12}$$

Applying $y = 0$

$$[x\cos\varphi - h\cos\varphi - k\sin\varphi]^2 + [-k\cos\varphi + x\sin\varphi - h\sin\varphi]^2 = R^2 \tag{13}$$

by substituting $h = r_e\cos\varphi, k = r_e\sin\varphi$

$$x^2 - 2r_e\cos\varphi x + r_e^2 - R^2 = 0. \tag{14}$$

Finally, solving for $x > 0$, we obtain

$$x = r_e\cos\varphi + \sqrt{R^2 - r_e^2\sin^2\varphi}. \tag{15}$$

The variable x represents the measurement output of our sensor. Therefore, we have to compensate for its values in order to find the real radial measurements. In the following, we calculate the correction coefficients to be applied to each harmonic in order to find the correct radial measurements.

The continuous component is given by

$$R = \frac{r_e^2}{4R} - \frac{3r_e^4}{64r^3}. \tag{16}$$

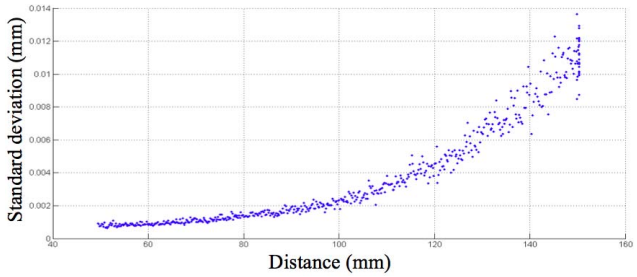

Fig. 9. Trend of measurement of the designed prototype.

The amplitude of first harmonic, that is the distance from the center of the pipe, is r_e, as expected.

The amplitude of the second harmonic is

$$\frac{r_e^2}{4R} = \frac{(A_{\text{first harmonic}})^2}{2R}. \tag{17}$$

And the amplitude of the third harmonic is

$$\frac{3r_e^4}{64R^3} = \frac{3(A_{\text{first harmonic}})^4}{64R^3}. \tag{18}$$

The second harmonic is in phase with the first harmonic in the sense that they have the maximum value of the cosine at the same point, and in this way can be easily subtracted from the measurement.

This procedure will be adopted in order to compensate for the measurement of the pipe circularity, realized by placing the rangefinder in the middle of the pipe and rotating the pipe around it.

V. Results

The resolution of the instrument was calculated through its standard deviation, and its trend depending on the distance of the object is presented in Fig. 9. It is possible to observe that with a measurement speed of 100 Hz a deviation of less than 10 μm was obtained up to 14 cm and less than 14 μm for the whole range. The system showed an accuracy of $\sim$25 μm on the single measurement.

These results are very satisfactory because the tests were carried out in the worst case: on a black surface, rough and not clean, taken from a real pipe.

In addition, to make an assessment of the final prototype, several acquisitions were made by mounting it on a setup comprising a motorized translation stage and a commercial laser rangefinder (Micro-Epsilon, OPTONCDT1401) based on the same principle of operation (triangulation) comparing their performances under the same conditions of measurement (temperature, vibration, etc.). In the graph of Fig. 10 a set of measurements is shown. The obtained sinusoidal shape is due to the slightly off-axis position of the mechanics compared with the pipe. The interesting aspect of this graph is that the designed instrument is more linear, as expected, than the commercial one used as reference for comparison (red line in Fig. 9).

Other measurements were done to characterize the rangefinder compared with a coordinate measurement machine (CMM) during a radial measurement of the pipe. Fig. 11 shows a comparison of the measurement given by

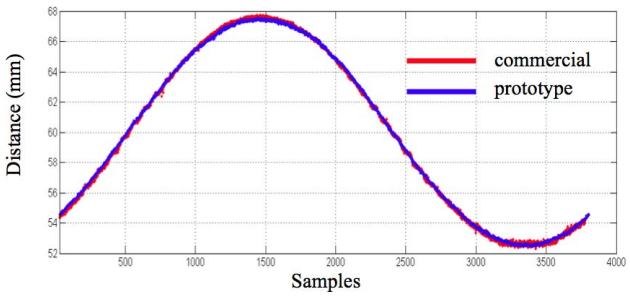

Fig. 10. Comparison of the designed rangefinder (blue line) with a commercial one (red line).

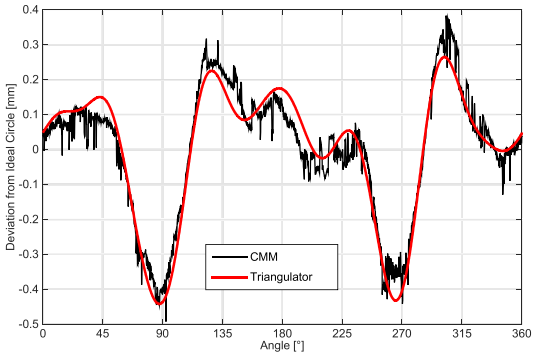

Fig. 11. Comparison of the designed rangefinder (red) with a CMM one (black).

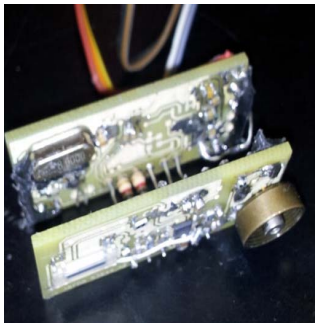

Fig. 12. Photo of the realized rangefinder.

our prototype, after the application of the mathematical compensation reported in Section IV, with the measurement output of a 3-D CMM, reported in polar coordinates. The rangefinder measurement is done on a great number of points (2500), and the output is filtered in order to highline the noncircularity of the pipe neglecting the surface roughness.

VI. Conclusion

The designed instrument (Fig. 12) has shown very good results in terms of resolution, less than 10 μm on the whole range, compactness, the dimensions are $4 \times 3.5 \times 2$ cm, very small for this kind of instrumentation, and cost, not more than \$60 to assemble one rangefinder. There is no other instrument of this kind available on the market at this price giving the same results in terms of accuracy. The error of nonlinearity does not exceed 50 μm over a range of 100 mm with

a minimum distance measured of 5 cm. The results obtained are very good compared with the commercial rangefinders, which have a cost of more than €1000 for comparable performances, but without the compactness of this design. The performances showed are very promising for developing an instrument to be used on a steel pipe production line as requested by Tenaris Dalmine, for measuring the eccentricity of the pipes.

ACKNOWLEDGMENT

The authors would like to thank A. M. G. Miralles for working on the prototype during her thesis.

REFERENCES

[1] S. Donati, *Electro-Optical Instrumentation: Sensing and Measuring With Lasers*, 1st ed. Englewood Cliffs, NJ, USA: Prentice-Hall, Apr. 2004.
[2] K.-E. Peiponen, R. Myllylä, and A. V. Priezzhev, *Optical Measurement Techniques*, 1st ed. Berlin, Germany: Springer-Verlag, Mar. 2009.
[3] E. Doebelin, *Measurement Systems: Application and Design*, 5th ed. New York, NY, USA: McGraw-Hill, Jun. 2003.
[4] R. S. Lu, Y. F. Li, and Q. Yu, "On-line measurement of the straightness of seamless steel pipes using machine vision technique," *Sens. Actuators A, Phys.*, vol. 94, nos. 1–2, pp. 95–101, Oct. 2001.
[5] C. P. Keferstein and M. Marxer, "Testing bench for laser triangulation sensors," *Sensor Rev.*, vol. 18, no. 3, pp. 183–187, 1998.
[6] R. G. Dorsch, G. Häusler, and J. M. Herrmann, "Laser triangulation: Fundamental uncertainty in distance measurement," *Appl. Opt.*, vol. 33, no. 7, pp. 1306–1314, 1994.
[7] J. Santolaria, D. Guillomía, C. Cajal, J. A. Albajez, and J. J. Aguilar, "Modelling and calibration technique of laser triangulation sensors for integration in robot arms and articulated arm coordinate measuring machines," *Sensors*, vol. 9, no. 9, pp. 7374–7396, 2009.
[8] M. Norgia, A. Pesatori, C. Svelto, A. De Marchi, M. Zucco, and M. Stupka, "High-resolution mode-locked laser rangefinder with harmonic downconversion," *IEEE Trans. Instrum. Meas.*, vol. 61, no. 5, pp. 1536–1542, May 2012.
[9] M. Norgia, A. Magnani, and A. Pesatori, "High resolution self-mixing laser rangefinder," *Rev. Sci. Instrum.*, vol. 83, no. 4, p. 045113, 2012.
[10] A. Magnani, A. Pesatori, and M. Norgia, "Real-time self-mixing interferometer for long distances," *IEEE Trans. Instrum. Meas.*, vol. 63, no. 7, pp. 1804–1809, Jul. 2014.
[11] F. Cavedo, A. Pesatori, M. Norgia, P. di Milano, and G. E. Solari, "Laser rangefinder for steel pipes characterization," in *Proc. I2MTC Conf.*, Pisa, Italy, May 2015, pp. 1387–1390.
[12] H. M. Merklinger, "The Scheimpflug's patent," *Photo Techn.*, vol. 17, no. 6, 1996.
[13] F. J. Pipitone and T. G. Marshall, "A wide-field scanning triangulation rangefinder for machine vision," *Int. J. Robot. Res.*, vol. 2, no. 1, pp. 39–49, Mar. 1983.

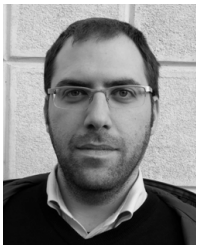

Federico Cavedo was born in Romano di Lombardia, Italy, in 1986. He received the bachelor's degree in electronics engineering and the M.Sc. degree in electronics engineering from the Politecnico di Milano, Milan, Italy, in 2009 and 2013, respectively.

He was a Post-Doctoral Researcher with the Opto-Electronic Measurement Group, Politecnico di Milano, until 2013. His current research interests include optical and electronic measurements, and measurement applications using microcontrollers or field-programmable gate array system.

Michele Norgia (S'99–M'01–SM'09) was born in Omegna, Italy, in 1972. He received the M.S. (Hons.) degree in electronics engineering and the Ph.D. degree in electronics engineering and computer science from the University of Pavia, Pavia, Italy, in 1996 and 2000, respectively.

He joined the Electronic and Information Science Department, Politecnico di Milano, Milan, Italy, in 2006, as an Assistant Professor of Electrical and Electronic Measurements. Since 2014, he has been an Associate Professor with the Politecnico di Milano. He has authored over 150 papers in international journals or international conference proceedings. His current research interests include optical and electronic measurements, interferometry, chaos in lasers, optical frequency standards, microelectromechanical sensors, biomedical measurements, and instrumentation.

Dr. Norgia is a member of the Association of the Italian Group of Electrical and Electronic Measurements.

Alessandro Pesatori (S'06–M'09) was born in Milan, Italy, in 1979. He received the M.Sc. degree in biomedical engineering from the Politecnico di Milano, Milan, in 2004, and the Ph.D. degree in information engineering from the Electronics and Information Science Department, Politecnico di Milano, in 2008.

He has been an Assistant Professor of Electrical and Electronic Measurements with the Politecnico di Milano since 2008. He has authored about 50 papers in international journals or international conference proceedings. His current research interests include optical and electronic measurements with biomedical applications, laser spectroscopy, methods of 2-D and 3-D analysis of biomedical images, and advanced automation systems.

Dr. Pesatori is a member of the Association of the Italian Group of Electrical and Electronic Measurements.

Gabriel E. Solari was born in Argentina. He received the Ingeniero Electrónico degree from the Universidad Nacional de Rosario, Rosario, Argentina, and the M.Sc. and Ph.D. degrees in applied sciences from the Centre for Systems Engineering and Applied Mechanics, Université catholique de Louvain, Louvain-la-Neuve, Belgium, in 2003 and 2005, respectively.

He was with SIDERCA, Campana, Argentina, a seamless steel tube company, from 1997 to 2001. He has been a Senior Control Engineer with Dalmine S.P.A., Dalmine, Italy, a big seamless tube manufacturer, specialized in casting plants and arc electric furnaces. His current research interests include process automation, practical applications of control theory, layout and logistic optimization, filter design, improvement of Proportional Integral Derivative controllers, identification, and electromagnetic phenomena.

Dr. Solari received a fellowship from the Belgian Government.